Zoosyst. Evol. 100 (2) 2024, 755–767 | DOI 10.3897/zse.100.118000

PENSOFT

MUSEUM FÜR NATURKUNDE BERLIN

A new rare catfish species from southeastern Brazil provides insights into the origins of similar colour patterns in syntopic, distantly related mountain trichomycterines (Siluriformes, Trichomycteridae)

Wilson J. E. M. Costa[1], Caio R. M. Feltrin[1], José Leonardo O. Mattos[1], Axel M. Katz[1]

1 *Laboratory of Systematics and Evolution of Teleost Fishes, Institute of Biology, Federal University of Rio de Janeiro, Caixa Postal 68049, CEP 21941-971, Rio de Janeiro, Brazil*

https://zoobank.org/C3BED28C-2D3A-416F-BEBA-73DF1BECA132

Corresponding author: Wilson J. E. M. Costa (wcosta@acd.ufrj.br)

Academic editor: Nicolas Hubert ♦ **Received** 30 December 2023 ♦ **Accepted** 2 April 2024 ♦ **Published** 11 June 2024

Abstract

Colour patterns are diverse in trichomycterine catfishes and are often used to diagnose species. Here, we analyse the first case of adults of two syntopic species of *Trichomycterus* sharing nearly identical colour patterns: a rare new species of the subgenus *Paracambeva* and *Trichomycterus maculosus*, a distantly related species of the subgenus *Trichomycterus*. Both species are endemic to the upper Rio Paraíba do Sul basin (RPSB), which had a different course until the Tertiary period and is situated within the Southeastern Brazilian Continental Rift, mostly active in the Eocene-Oligocene. A time-calibrated multigene analysis, 3144 bp, supported the new species as sister to *Trichomycterus itatiayae*, both comprising a lineage with Middle Miocene age, when that colour pattern would have first arisen. The new species is diagnosed by characters from the latero-sensory system and bone morphology. Our results, combined with available biogeographical data, indicated the colour pattern of *T. maculosus* arising in the Late Pliocene, following the dispersal of its group to the upper RPSB after river course changing. Two hypotheses for the independent origin of the same colour pattern are discussed. First, a case of evolutionary convergence for adaptation to live on a similarly coloured gravel substrate, giving some cryptic advantage against predators. Second, mimetic association through anti-predation features. In the latter case, although trichomycterids lack fin spines to inoculate venom as in other catfishes, the species here studied have a supposed axillary gland above the pectoral fin, just posterior to the opercular odontodes, but with properties and functions still unknown.

Key Words

Atlantic forest, molecular systematics, mountain biodiversity, Rio Paraíba do Sul basin, Serra da Mantiqueira

Introduction

Colouration has an important role in the biology of teleost fish species, involving attributes related to their behaviour and ecology (e.g., Price et al. 2008). Colour patterns are particularly diverse among the Trichomycterinae (Eigenmann 1918), one of the most diverse groups of Neotropical catfishes, and as a consequence, they have been frequently used to diagnose species and groups since the 19th century (Valenciennes 1832). During field studies, colour patterns are often the primary tool to distinguish sympatric trichomycterine species, although chromatic polymorphism within species is not uncommon (Arratia et al. 1978; Sarmento-Soares et al. 2005; da Silva et al. 2010; Costa et al. 2023a; Vilardo et al. 2023). On the other hand, the occurrence of sympatric, non-closely related trichomycterine species exhibiting identical colour patterns is a rarely reported event (Costa et al. 2020a; Reis et al. 2020). The only report of two distantly related trichomycterines with the same colour pattern and found sharing the same habitat was made by Barbosa and Costa (2008) for *Trichomycterus itatiayae* Miranda Ribeiro, 1906, a species of the subgenus *Paracambeva* Costa, 2021, and *Trichomycterus nigroauratus* Barbosa & Costa, 2008 of the subgenus *Trichomycterus* (Costa 2021).

Herein we first report a rare new trichomycterine catfish species, with only four specimens found in the last two collections of six collecting trips between 1991 and 2023 to the upper Rio do Peixe drainage, Rio Paraíba do Sul basin (hereafter RPSB), southeastern Brazil. This species is morphologically similar to the syntopic *Trichomycterus maculosus* Barbosa & Costa, 2010, which is sister to *T. nigroauratus*. Specimens of this new species had a colour pattern approximately identical to that exhibited by larger adult specimens above 70 mm SL of *T. maculosus* (small spots on the dorsal part of the flank and a narrow dark grey longitudinal stripe along the flank midline; see description and included illustrations below), found in the same habitat (i.e., over gravel stream bottom). The two species are externally distinguishable by a few characters, comprising the relative position of the dorsal and anal fins, with the anal-fin origin positioned at a vertical line through the posterior-most portion of the dorsal-fin base in *T. maculosus*, vs. at a vertical line just posterior to the middle of the dorsal-fin base in the new species; number of pectoral-fin rays, eight in *T. maculosus* vs. seven in the new species; and body depth, with *T. maculosus* being more slender than the new species, reaching 12.8–13.8% of the standard length (SL) in *T. maculosus*, vs. 16.6–20.0% SL in the new species. Preliminary analysis in the laboratory revealed that the new species is sister to *T. itatiayae*, a member of *Paracambeva*, thus contrasting with the syntopic *T. maculosus*, a common species endemic to the upper Rio do Peixe drainage, belonging to the *Trichomycterus nigroauratus* group of the subgenus *Trichomycterus* (Barbosa and Costa 2010; Costa 2021). *Paracambeva* is diagnosed by an anterior infraorbital canal not attached to the lacrimal, a relatively short interopercle, and a relatively slender parapophysis of the second free vertebra (Costa 2021).

The new species and *T. maculosus* are only known from streams belonging to the upper Rio do Peixe drainage, Rio Paraiba do Sul basin (hereafter RPSB), in the southern plateau of the Serra da Mantiqueira, a mountain range that is an important centre of biodiversity in the Atlantic Forest, with a great concentration of endemic trichomycterines of the genus *Trichomycterus* Valenciennes, 1832 (e.g., Costa and Katz 2021). The origin of the southern plateau of the Serra da Mantiqueira is related to an uplift during the Neo-Cretaceous as a result of the process of separation of the South American and African plates (Riccomini et al. 2004, 2010). The southern plateau of the Serra da Mantiqueira is presently a divisor between the Rio Paraná basin and the RPSB. Geological evidence indicates that the upper portion of the present RPSB, including all the area today inhabited by the new species *T. itatiayae*, *T. maculosus*, and *T. nigroauratus* between the Neo-Cretaceous and the Tertiary, had a different course, directed to the northwest and being connected to the Rio Tietê drainage, the Rio Paraná basin, instead of the middle and lower sections of the RPSB (King 1956; Riccomini et al. 2010). In addition, the Rio do Peixe drainage is situated in a core area of the region known as the South-eastern Brazilian Continental Rift, which had its greatest development in the Eocene-Oligocene, including the paleo-lake Tremembé formed during the Oligocene (e.g., Riccomini et al. 2004, 2010). The objectives of the present study are to describe the new species, perform a time-calibrated analysis to test the positioning of the new species, and infer the timing of the origin of derived colour patterns in both lineages using a biogeographical temporal context.

Materials and methods

Specimens

Field procedures were approved by CEUA-UFRJ (Ethics Committee for Animal Use of the Federal University of Rio de Janeiro; permit numbers: 065/18 and 084/23) and collecting permits were given by ICMBio (Instituto Chico Mendes de Conservação da Biodiversidade; permit number: 38553-11). For details about specimen euthanasia, fixation, and conservation, see Costa et al. (2023b). Specimens were deposited in the ichthyological collection of the Instituto de Biologia, Universidade Federal do Rio de Janeiro (UFRJ). Comparative material is listed in Barbosa and Costa (2008), Costa and Katz (2021), and Costa et al. (2023b). A complete list of specimens used in morphological comparisons, with their respective catalogue numbers and locality coordinates, appears in Suppl. material 1.

Morphological data

Methods for taking and describing morphological characters were according to recent studies on *Paracambeva*, including morphometric and meristic data following Costa (1992) and Costa et al. (2020b), osteological preparations following Taylor and Van Dyke's (1985), latero-sensory system nomenclature following Arratia and Huaquin (1995) and Bockmann and Sazima (2004), bone terminology following Costa (2021) and Kubicek (2022), and fin ray formulae following Bockmann and Sazima (2004).

DNA extraction, amplification, and sequencing

Methods for DNA extraction, amplification, and sequencing followed the most recent phylogenetic analysis of *Paracambeva* (Costa et al. 2023b), with PCR reactions performed in 45 µl with the following reagent concentrations: 5× GreenGoTaq Reaction Buffer (Promega), 1.0 mM $MgCl_2$, 1 µM of each primer, 0.2 mM of each dNTP, 1 u of Promega GoTaq Hot Start polymerase, and 50 ng of total genomic DNA; thermal profile: 95 °C for 5 min; 35 cycles of 94 °C for 1 min; 50–60 °C for 1–1.5 min;

and 73 °C for 7 min; sequencing reactions performed in 20 µL reaction volumes containing 4 µL BigDye, 2 µL sequencing buffer 5× (Applied Biosystems), 2 µL of the PCR products (30–40 ng), 2 µL primer, and 10 µL ultrapure water; and the thermal profile was 35 cycles of 30 s at 95 °C, 30 s at 55 °C, and 1.5 min at 73 °C. Primers used for mitochondrially encoded genes were: Cytb Siluri F and Cytb Siluri R (Villa-Verde et al. 2012) for *cytochrome b* (CYTB); FISHF1 and FISHR1 (Ward et al. 2005) for *cytochrome c oxidase I* (COX1). Primers for the nuclear encoded genes were: MYH6 TRICHO F and MYH6 TRICHO R (Costa et al. 2020c) for *myosin heavy chain 6* (MYH6), and RAG2 TRICHO F and RAG2 TRICHO R (Costa et al. 2020c) for *recombination activating 2* (RAG2). MEGA 11 (Tamura et al. 2021) was used to read and interpret sequencing chromatograms, to perform the sequence annotation, and to translate DNA sequences into amino acid residues to verify the absence of premature stop codons or indels. GenBank accession numbers are in Table 1.

Phylogenetic analyses

The terminal taxa for the phylogenetic analyses include all species of *Paracambeva*, including the new species herein described, and all species of the subgenus *Trichomycterus*. The remaining species of *Trichomycterus* and outgroups included in the analysis are the same as those used in Costa et al. (2023b). See Costa et al. (2023b) for justification for outgroup selection. Each gene dataset was aligned using the Clustal W algorithm (Chenna et al. 2003) implemented in MEGA 11 and analysed for determination of the optimal partitioning and evolutionary models (Table 2) using the Corrected Akaike Information (AICc) in PartitionFinder 2.1.1 (Lanfear et al. 2016). Phylogenetic analyses followed the methods described in Costa et al. 2023b), comprising Bayesian Inference performed with Beast 1.10.4 (Suchard et al. 2018), using the Yule process as the tree prior (Gernhard, 2008), two independent Markov chain Monte Carlo (MCMC) runs with 9×10^7 generations with a

Table 1. Terminal taxa and GenBank accession numbers by gene used in molecular analyses.

	COI	CYTB	RAG2	MYH6
Diplomystes nahuelbutaensis	AP012011.1	MN640590	DQ492317	–
Callichthys callichthys	MZ051783.1	KP960058	DQ492324	–
Corydoras panda	NC049097.1	NC049097.1	KP960362.1	–
Nematogenys inermis	EU359428	–	KY858182.1	KY858107.1
Trichogenes longipinnis	OQ810037	MK123704	MF431117	MF431104.1
Microcambeva ribeirae	MN385807.1	OK334290	MN385832	MN385819.1
'Trichomycterus' areolatus	AP012026.1	FJ772214	KY858188	–
Ituglanis boitata	OQ810038	MK123706	MK123758	MK123734.1
Cambeva barbosae	MK123689	MK123713	MN385820	MK123740.1
Scleronema minutum	MK123685	MK123707	MK123759.1	KY858109.1
Trichomycterus nigricans	MN813005.1	MT470415.1	MK123765.1	MK123750.1
Trichomycterus albinotatus	MN813007.1	MT459172.1	MN812990.1	MK123743.1
Trichomycterus brasiliensis	MT470418.1	MT470418.1	MK123763.1	MK123744.1
Trichomycterus itatiayae	MW671552	MW679291	OR995282	OL779229
Trichomycterus reinhardti	MK123698.1	MK123727.1	MK123698.1	MF431106.1
Trichomycterus funebris	MT941786.1	MT941823.1	KY858194	KY858121
Trichomycterus pauciradiatus	MT941796	MT941833	MW196782	MW196769.1
Trichomycterus ingaiensis	MT941790	MT941829	OR995283	–
Trichomycterus piratymbara	KY857970	KY858040	KY858121	KY858194
Trichomycterus sainthilairei	MT941814	MT941851	OR995284	–
Trichomycterus septemradiatus	MK123700	MK123729	MW196781	MK123755.1
Trichomycterus humboldti	MT941787	MT941824	OR995285	–
Trichomycterus luetkeni	MT941793	MT941831	KY858214	KY858148
Trichomycterus anaisae	MT941782	MT941820	OR995286	–
Trichomycterus coelhorum	OR981611	OQ660192	OQ660183	–
Trichomycterus adautoleitei	OR981612	OQ660193	–	–
Trichomycterus antiquus	OR981613	OR995280	OR995287	–
Trichomycterus giganteus	MK123693.1	MK123720	MT446426	MK123746.1
Trichomycterus maculosus	MN813010.1	OR995281	MN812994.1	MN812998.1
Trichomycterus nigroauratus	MK123696	OK247569	MK123766	MK123751.1
Trichomycterus quintus	MT299917.1	MN812999	–	MT305242.1
Trichomycterus mutabilicolor	OR981614	OK247576	–	–
Trichomycterus santaeritae	MN813009	MN813001	MN812993	MN812997
Trichomycterus immaculatus	MK123694	MK144348	MF431120	MK123747
Trichomycterus santaeritae	MN813009	MN813001	MN812993	MN812997

Table 2. Best-fitting partition schemes with the respective number of base pairs and the best-suited evolutionary models.

Partition	Base pairs	Evolutive Model
COX1 3rd	251	TRN+I+G
COX1 1st	251	TRN+I+G
COX1 2nd, CYTB 2nd	594	GTR+I+G
CYTB 3rd	343	GTR+G
CYTB 1st	343	GTR+I+G
RAG2 2nd, RAG2 1st	546	SYM+G
RAG2 3rd	273	GTR+G
MYH6 1st	181	GTR+G
MYH6 2nd	181	TRN
MYH6 3rd	181	K80+G

sampling frequency of 1000; determination of the convergence of the MCMC chains and the proper burn-in values through the stationary phase of the runs using the effective sample size analysed with Tracer 1.7.1 (Rambaut et al. 2018), combination of generated trees using LogCombiner v.1.10.4 (Suchard et al. 2018) following a 25% burn-in at the outset of each run, and calculation of the consensus tree and Bayesian posterior probabilities using Tree Annotator version 1.10.4 (Suchard at al., 2018); and Maximum Likelihood analysis performed with IQTREE 2.2.2.6 (Minh et al. 2020), with support node expressed by ultrafast bootstrap (Hoang et al. 2018) and the Shimodaira-Hasegawa-like approximate likelihood ratio test (SH-aLRT; Guindon et al. 2010), both using 1000 replicates. In order to evaluate the contribution of each genetic locus dataset analysed, we generated individual trees for each of the nuclear genes and one for the mitochondrial genes, using ML as above described.

Divergence-time estimation

The divergence time analysis was conducted in Beast 1.10.4 using the same dataset, partitions, evolution models, and parameters as described above. Additionally, the analysis incorporated a lognormal uncorrelated relaxed clock model and a Yule speciation process as the tree prior (Gernhard 2008). Calibration points were established as follows: the origin of the Trichomycteridae with a normal prior distribution (mean = 106 MA, SD = 5.0), following the estimative of Betancur-R et al. (2015), which is often used as an indirect calibration strategy in other studies on trichomycterids (e.g., Ochoa et al. 2017; Vilardo et al. 2023); and the origin of the genus *Corydoras* with a lognormal prior distribution (mean = 55 MA, SD = 1), based on the dating of *Corydoras revelatus* Cockerell, 1925, the oldest known fossil of callichthyid catfishes. MCMC chains were assessed to verify convergence by evaluating the effective sample size of the runs in Tracer 1.7.1. The time-scaled tree was obtained using Tree Annotator version 1.10.4 to generate the consensus tree.

Results

Taxonomic accounts

Trichomycterus (*Paracambeva*) *antiquus* sp. nov.

https://zoobank.org/

Figs 1–3, Table 3

Type material. ***Holotype*.** Brazil • 1 ex., 72.2 mm SL; Estado de São Paulo: Município de São José dos Campos: small stream tributary of the Rio Santa Bárbara, Rio do Peixe drainage, Rio Paraíba do Sul basin, São Francisco Xavier, Serra dos Poncianos, part of the Serra da Mantiqueira; 22°51'47"S, 45°54'60"W; about 980 m asl; 21 April 2023; C.R.M. Feltrin, leg.; UFRJ 13674.

***Paratypes*.** (all from Estado de São Paulo: Município de São José do Campos: Rio do Peixe drainage, Rio Paraíba do Sul basin, São Francisco Xavier, Serra dos Poncianos, part of the Serra da Mantiqueira): BRAZIL • 1 ex., 75.6 mm SL (stained with alizarin and partially dissected); collected with holotype; UFRJ 13673; 1 ex., 79.1 mm SL; stream tributary of Rio Santa Bárbara; 22°53'45"S, 45°56'34"W; about 765 m asl; same collector and date as holotype; UFRJ 13681; 1 ex., 44.5 mm SL (cleared and stained for osteological analysis); same locality and collector as holotype; 29 October 2023; UFRJ 14201.

Diagnosis. *Trichomycterus antiquus* is distinguished from all other species of *Paracambeva*, except *T. itatiayae*, by having a relatively large head, its length 20.4–22.8% SL (vs. 11.4–18.1% SL), the presence of a deep concavity on the postero-ventral margin of the metapterygoid, accommodating a pronounced expansion of the postero-dorsal quadrate outgrown (Fig. 3B, see also Costa 2021: fig. 3B for similar condition in *T. itatiayae*; vs. metapterygoid concavity, when present, never deep and quadrate expansion, when present, never pronounced in other species of *Paracambeva*, e.g. Costa et al. 2023b: figs. 6G, H) and the presence of a a deep U-shaped concavity on the dorsal margin of the anterior hyomandibular anterior outgrown (Fig. 3B, see also Costa 2021: fig. 3B for similar condition in *T. itatiayae*; vs. concavity, when present, never U-shaped, e.g. Costa et al. 2023b: figs. 6G, H). *Trichomycterus antiquus* differs from *T. itatiayae* by the presence of the anterior infraorbital canal (vs. absence), jaw teeth sharply pointed (vs. incisiform), a wider body and head (body width 11.9–15.0 vs. 6.2–8.8% SL; head width 51.8–58.4 vs. 68.7–75.7% SL), a longer pre-dorsal length (66.0–65.2 vs. 59.2 – 64.0% SL), a longer pre-pelvic length (60.7– 65.2 vs. 54.9–56.9% SL), a deeper head (head depth 51.5–58.4 vs. 39.0–50.8% SL), a large eye (eye diameter 8.8–11.3 vs. 7.4–8.2% of the head length), a short sesamoid supraorbital, about twice longer than the lacrimal (Fig. 3A; vs. long, about four times longer, Costa 2021: fig. 2B); a well-developed postero-lateral process of the autopalatine (Fig. 3A; vs. rudimentary, Costa 2021: fig. 2B); and a slender and long maxilla, longer than premaxilla (Fig. 3A; vs. relatively deep, shorter than premaxilla, Costa 2021: fig. 2B).

Figure 1. *Trichomycterus* (*Paracambeva*) *antiquus* sp. nov., UFRJ 13674, holotype, 72.2 mm SL. **A.** Left lateral view; **B.** Dorsal view; **C.** Ventral view.

Description. ***General morphology.*** Morphometric data appear in Table 3. Body relatively deep (Fig. 1A), greatest body depth at vertical through midway between pectoral and pelvic-fin bases. Trunk subcylindrical to compressed on caudal peduncle, dorsal and ventral lateral profiles weakly convex to almost straight. Whole body, except venter, covered with minute papillae. Small putative axillary gland above pectoral fin, below lateral line, with small orifice just posterior to opercular patch of odontodes (Fig. 2A). Lateral line of trunk consisting of anterior minute canal with two pores obliquely arranged, posterior followed by almost imperceptible line between humeral region and caudal-fin base with minute superficial neuromasts. Anterior-most pore of lateral line more ventrally positioned than posterior one. Urogenital opening consisting of transverse aperture situated in shallow depression. Anus positioned immediately in front of urogenital opening, at vertical just posterior to dorsal-fin origin.

Head sub-trapezoidal in dorsal view, dorsal surface flat (Fig. 1B). Eye small, positioned on dorsal head surface, nearer snout tip than posterior margin of opercle. Distance between anterior and posterior nostrils approximately

Table 3. Morphometric data of *Trichomycterus antiquus* sp. nov.

	Holotype	Paratypes (n=3)
Standard length (SL)	72.2	44.5–79.1
Percentage of standard length		
Body depth	20.0	16.1–18.1
Caudal peduncle depth	14.7	12.1–14.9
Body width	17.3	11.9–15.0
Caudal peduncle width	6.0	4.0–8.1
Pre-dorsal length	68.1	66.0–68.5
Pre-pelvic length	62.4	60.7–65.2
Dorsal-fin base length	10.5	10.1–12.0
Anal-fin base length	10.1	9.2–10.3
Caudal-fin length	15.3	13.1–17.6
Pectoral-fin length	10.5	12.1–13.9
Pelvic-fin length	8.2	8.2–9.2
Head length	22.8	20.4–22.1
Percentage of head length		
Head depth	52.2	51.5–58.4
Head width	90.8	85.7–90.2
Snout length	52.3	40.4–49.5
Interorbital width	26.9	24.5–28.1
Preorbital length	13.8	15.5–16.1
Eye diameter	9.8	8.8–11.3

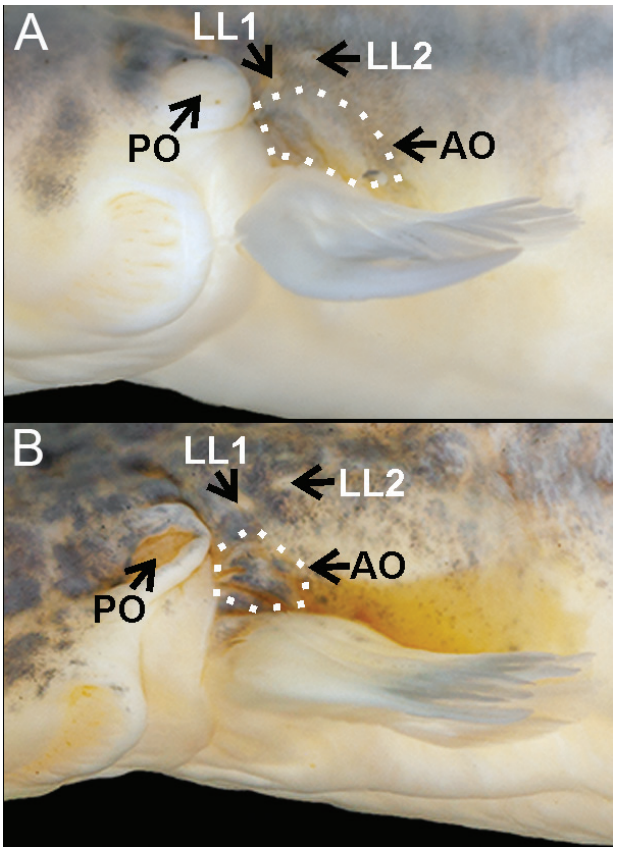

Figure 2. Lateral view of the head, left side, of **A.** *Trichomycterus* (*Paracambeva*) *antiquus* sp. nov., UFRJ 13674, holotype, 72.2 mm SL; **B.** *Trichomycterus* (*Trichomycterus*) *maculosus*, UFRJ 13676, 97.6 mm SL. AO, supposed axillary organ; LL 1–2, lateral line pores 1–2; PO, preopercular patch of odontodes.

half distance between posterior nostril and orbit. Tip of nasal barbel posteriorly reaching area between orbit and opercular patch of odontodes, tip of maxillary and rictal barbels reaching middle of interopercular patch of odontodes. Mouth subterminal. Jaw teeth pointed, irregularly arranged. Cleared and stained specimen with 48 teeth on premaxilla, 38 on dentary. Odontodes narrow, pointed to sub-incisiform in larger odontodes of larger specimens, about straight, irregularly arranged, 14 or15 on opercle and 44 or 45 on interopercle. Cephalic latero-sensory system comprising long canal interconnecting supraorbital, posterior section of infraorbital, and postorbital canals, and isolated anterior infraorbital canal. Supraorbital sensory canal with three pores, s1, s3, and s6; anterior section of infraorbital canal with two pores, i1 and i3; posterior section of infraorbital canal with two pores, i10 and i11; and postorbital canal with two pores, po1 and po2. All pores paired. Pore s6 about equidistant from orbit than its homologous pore.

Fins thin with thick bases and convex free margins (Fig. 1A). Anal-fin origin at vertical, immediately posterior to middle of dorsal-fin base, at vertical through base of 4th bifid dorsal-fin ray. First pectoral-fin ray terminating in short filament, its length about 20% of pectoral-fin length. Pelvic posteriorly overlapping anus and urogenital papilla. Posterior extremity of pelvic fin at vertical through area just anterior to middle of dorsal-fin base. Pelvic-fin bases medially separated by minute interspace. Caudal fin subtruncate. Total dorsal-fin rays 11 (ii + II + 7), total anal-fin rays 9 (ii + II + 5), total pectoral-fin rays 7 (I + 6), total pelvic-fin rays 5 (I + 4), total principal caudal-fin rays 13 (I + 11 + I), total caudal dorsal procurrent rays 15 (xiv + I), total caudal ventral procurrent rays 13 (xii + I).

***Osteology* (Fig. 3).** Mesethmoid slender, T-shaped, anterior margin about straight, cornu narrow, longitudinal main axis gently laterally widening close anterior margin of lateral ethmoid. Lateral ethmoid without lateral projections. Lacrimal thin, not associated to infraorbital canal, separated from sesamoid supraorbital by long interspace. Sesamoid supraorbital short and slender, its length about twice lacrimal length, its width about equal lacrimal width. Premaxilla sub-trapezoidal in dorsal view, slightly tapering laterally. Maxilla slender, boomerang-shaped, slightly longer than premaxilla.

Autopalatine robust, sub-rectangular in dorsal view when excluding postero-lateral process, its largest width about half autopalatine length including anterior cartilage. Lateral margin of autopalatine nearly straight, medial margin concave. Autopalatine posterolateral process well-developed, triangular, its length about equal autopalatine length, excluding anterior cartilage. Metapterygoid subtrapezoidal, deeper than long. Postero-ventral margin of metapterygoid deeply concave, accommodating pronounced dorsal expansion of quadrate. Dorsal extremity of metapterygoid truncate, anterior margin convex, posterior margin about straight. Quadrate L-shaped, with pronounced postero-dorsal outgrowth, anterior margin concave. Hyomandibula moderately long. Anterior hyomandibular outgrowth deep, antero-dorsal margin about horizontal, posteriorly followed by deep U-shaped concavity.

Opercle elongate, slightly longer than interopercle. Dorsal opercular process short and blunt. Opercular articular facet for hyomandibula laterally protected by laminar shield articular facet for preopercle inconspicuous. Opercular odontode patch moderately slender, its width about half length of dorsal hyomandibula articular facet. Interopercle moderate in length, about equal hyomandibular anterior outgrowth length. Anterior margin of interopercle with pronounced anterior projection. Preopercle slender, without distinctive ventral projections.

Parurohyal lateral process relatively short, with blunt extremity, slightly curved posteriorly. Parurohyal head well-developed, with pronounced anterolateral paired process. Middle parurohyal foramen large, longitudinally elongate. Posterior process of parurohyal long, its length about four fifths distance between anterior margin of parurohyal and anterior insertion of posterior process. Branchiostegal rays 8.

Vertebrae 38. Ribs 15. Dorsal-fin origin at vertical through centrum of 21st vertebra, anal-fin origin at vertical through centrum of 24th vertebra. Two dorsal hypural plates

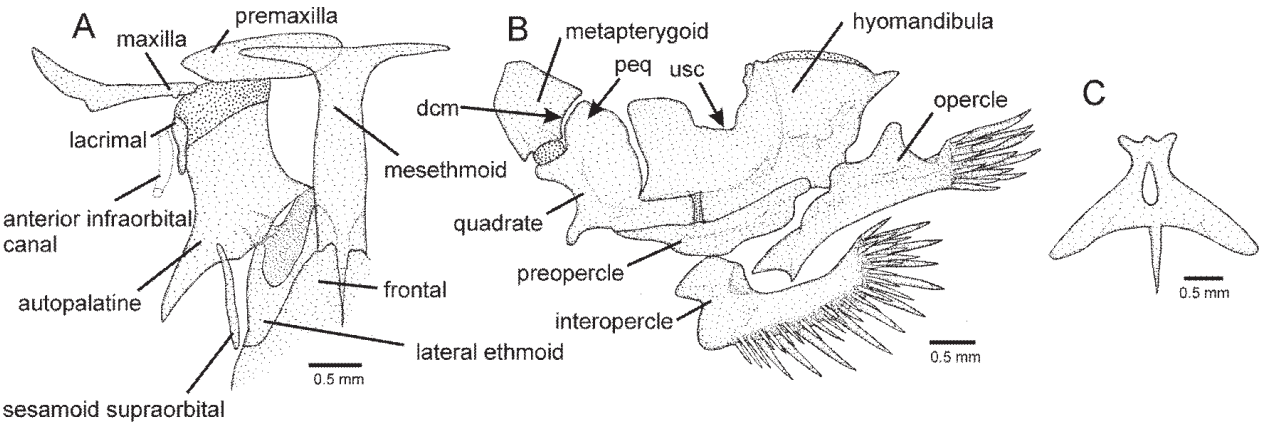

Figure 3. Osteological structures of *Trichomycterus* (*Paracambeva*) *antiquus* sp. nov. **A.** Mesethmoidal region and adjacent structures, left and middle portions, dorsal view; **B.** Left jaw suspensorium and opercular series, lateral view; **C.** Parurohyal, ventral view. Larger stippling represents cartilaginous areas. Abbreviations: dcm, deep concavity on the postero-ventral margin of the metapterygoid; peq, pronounced expansion of the postero-dorsal quadrate outgrown; usc, deep U-shaped concavity on the dorsal margin of the anterior hyomandibular anterior outgrown.

corresponding to hypurals 3 + 4 + 5; single ventral hypural plate corresponding to hypurals 1 + 2 + parhypural.

Colouration in alcohol. Flank pale yellow to yellowish white ventrally, with diffuse dark grey stripe along longitudinal midline, widening and breaking into small spots posteriorly. Great concentration of small dark grey spots on dorsal portion of flank, no or few similar spots on ventral portion. Dorsal surface of trunk and head pale brown, with small, faint grey spots, ventral surface white. Nasal and maxillary barbels pale brown, rictal barbel white. Fins hyaline, with whitish bases. In specimen UFRJ 13681, longitudinal stripe broader and darker, brown spots on dorsum, dorsal, and ventral portions of flank.

Etymology. From the Latin *antiquus* (old), referring to the relatively old estimated age of the species lineage in the Miocene (see below), when compared with the major species diversification of *Paracambeva* in the Pliocene.

Distribution. *Trichomycterus antiquus* is only known from the upper Rio do Peixe drainage, Rio Paraíba do Sul basin, south-eastern Brazil, at altitudes between about 765 and 980 m asl (Fig. 4).

Positioning of *Trichomycterus antiquus* and time-calibrated analysis

All phylogenetic analyses resulted in identical tree topologies (Fig. 5), in which *T. antiquus* is supported as sister to *T. itatiayae*, a species endemic to another region of the RPSB, with broad occurrence in streams draining the Maciço de Itatiaia, a massif forming a distinct nucleus of the Serra da Mantiqueira, and the adjacent Serra da Bocaina (Fig. 4). The clade comprising *T. antiquus* and *T. itatiayae*, hereafter the *Trichomycterus itatiayae* group, is supported as sister to a clade comprising all other species of *Paracambeva* known as the *T. reinhardti* species group (Costa 2021; Costa and Katz 2021). The independent analysis of individual gene trees indicated that all loci collaborated for this topology, since all gene trees corroborated monophyly of *Paracambeva* and both the RAG2 tree and the mitochondrial locus tree corroborated monophyly of the clade comprising *T. antiquus* and *T. itatiayae*, which is supported in both trees as sister to a clade comprising the remaining species of *Paracambeva* (Suppl. material 2). The age of the *Paracambeva* lineage was estimated at about 24.5 Ma, Late Oligoceno (95% HPD age interval 15.68–36.01), whereas according to the analysis, the divergence between the *T. itatiayae* group and the *T. reinhardti* group occurred at about 14.9 Ma, Middle Miocene (95% HPD age interval 7.16–24.84), and between *T. antiquus* and *T. itatiayae* at about 9.8 Ma, Late Miocene (95% HPD age interval 4.74–16.87).

Temporal origin of similar colour patterns

The presence of a broad black longitudinal stripe along the midline of the flank in juveniles, which often gradually becomes diffuse and fragmented into small spots in adults, combined with dark spots on the dorsum, occurs in most species of *Paracambeva* (Costa 2021; Costa and Katz 2021; Costa et al. 2023b), as well as in most species of the *T. nigroauratus* group of the subgenus *Trichomycterus* (e.g., Barbosa and Costa 2008; Costa et al. 2022). However, the specific colour pattern described here for *T. antiquus* and *T. maculosus* above about 70 mm SL, including a narrow stripe that posteriorly breaks into small spots, combined with the scarcity or absence of dark spots on the ventral part of the flank, occurs only in these two species and in *T. itatiayae* (Barbosa and Costa 2008: fig. 5). According to our analysis, this specific pattern would have first appeared in the ancestor of the clade comprising *T. antiquus* and *T. itatiayae*, around 14.9 Ma (95% HPD age interval 8.87–23.64), and a second time in the exclusive ancestor of *T. maculosus*, around 2.3 Ma (95% HPD age interval 0.85–4.56) (Fig. 5; Suppl. material 3).

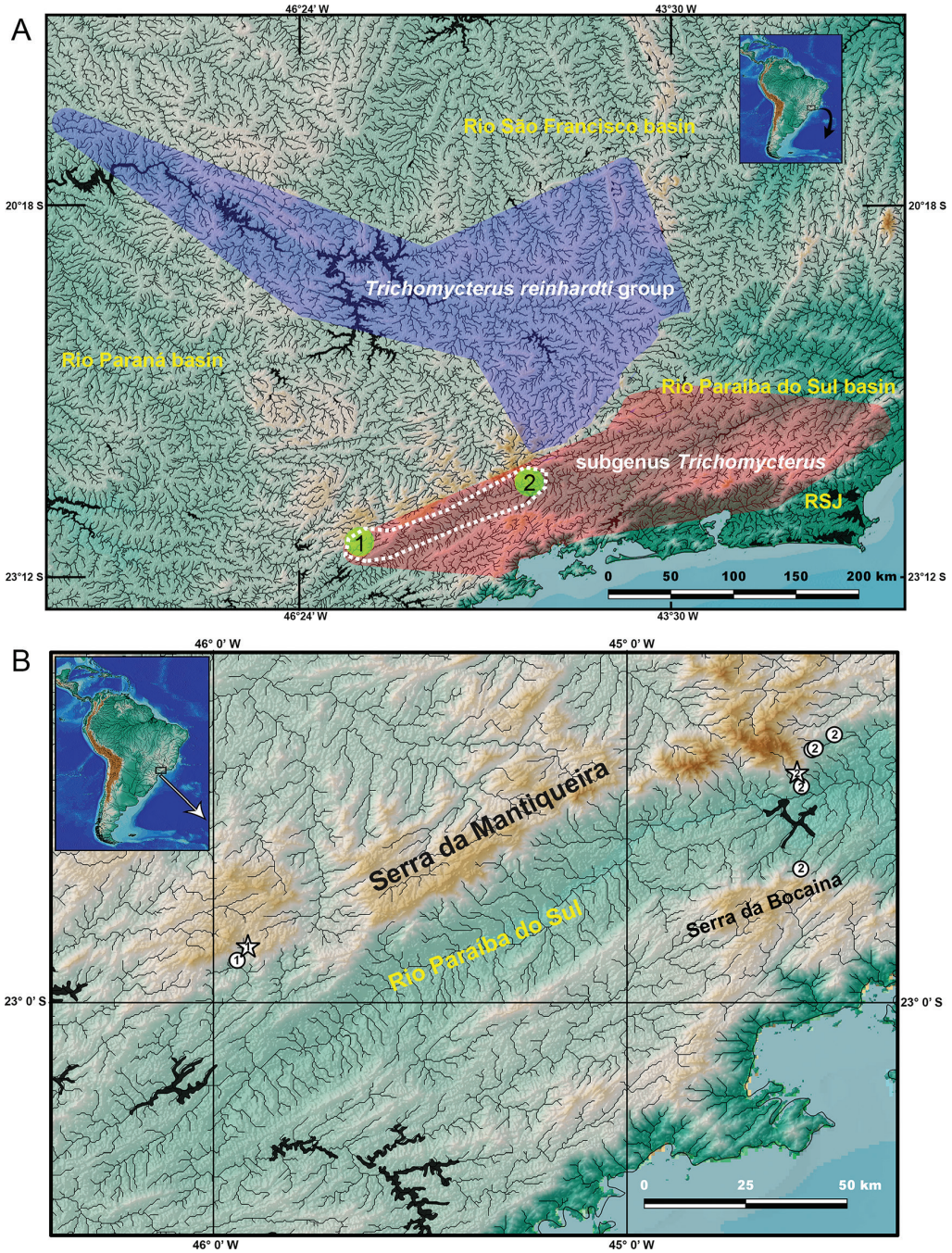

Figure 4. Map of south-eastern Brazil, showing: **A.** Geographical distribution of the *Trichomycterus* (*Paracambeva*) *itatiayae* group (delimited by a white dotted line), the *Trichomycterus* (*Paracambeva*) *reinhardti* group, and the subgenus *Trichomycterus*; **B.** collecting sites of 1, *Trichomycterus* (*Paracambeva*) *antiquus* sp. nov., and 2, *Trichomycterus* (*Paracambeva*) *itatiayae*. RSJ means Rio São João; stars indicate type localities.

Discussion

Temporal diversification and biogeographical context

According to a recent biogeographical analysis, the most recent common ancestor of *Paracambeva* lived in an area presently occupied by the upper Rio Paraná, upper Rio São Francisco, and Rio Paraíba do Sul basins (Vilardo et al. 2023). Presently, *Paracambeva* occupies a large region encompassing these three basins, with the *T. itatiayae* group occurring in a portion of the RPSB between the Rio do Peixe and the area close to the Serra da Bocaina and the *T. reinhardti* group occurring in a broad area of the upper Rio Paraná and upper Rio São Francisco basins (Fig. 4). Timing estimates support a Late Oligocene origin for the *Paracambeva* lineage and a Middle Miocene age for the split between the *T. itatiayae* and *T. reinhardti* groups (Fig. 5). Despite conclusive hypotheses about the time of origin of the present configuration of these basins that are not yet available, geological data point to a past connection between the upper section of the Rio Paraíba

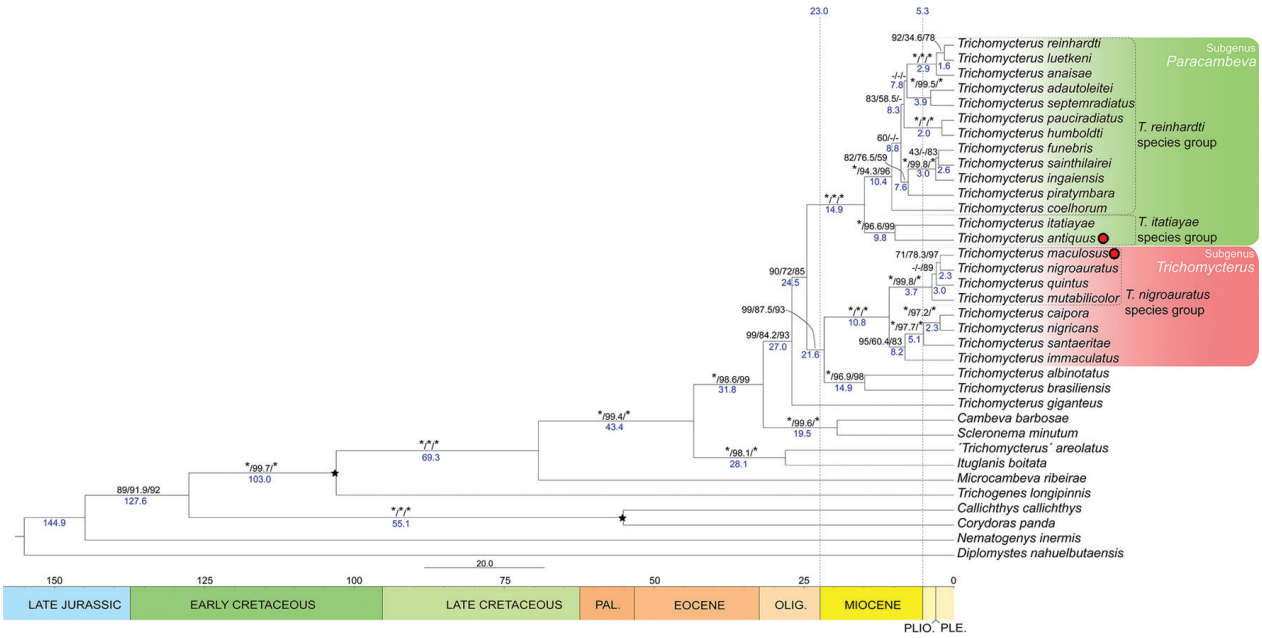

Figure 5. Time-scaled tree obtained from the Bayesian analysis in Beast for 28 species of Trichomycteridae and 4 species as outgroups, using a multigene data set (COX1, CYTB, RAG2, and MYH6 with a total of 3144 bp). Asterisks (*) indicate maximum support values, and dashes (-) indicate support values below 50. Black stars indicate the calibration points, and the coloured bars below the tree represent the geological epochs. Numbers above branches indicate posterior probabilities of the Bayesian Inference, followed by SH-aLRT support (%) and ultrafast bootstrap support (%) of the Maximum Likelihood (ML) analysis; blue numbers below nodes indicate its median age; Red dots after species names indicate the syntopic species discussed in this paper.

do Sul, above the area close to the Serra da Bocaina, and the Rio Paraná basin (King 1956; Riccomini et al. 2010), and between the upper section of the latter basin and the upper section of the Rio São Francisco basin (Rezende et al. 2018). Therefore, the present distribution of *Paracambeva* and our estimates for the time of origin of this subgenus fit into this model of river basin evolution, with the rupture between the upper Paraíba do Sul and the Paraná-São Francisco basin that would have occurred in the Paleogene (Riccomini et al. 2010) corresponding to the divergence between the *T. itatiayae* and *T. reinhardti* groups, which preceded the rupture of the connection between the upper Rio Paraná and upper Rio São Francisco basins during the Middle Miocene (Rezende et al. 2018), corresponding to the wide distribution of the *T. reinhardti* group in these basins (Fig. 4; Costa and Katz 2021).

On the other hand, temporal estimates indicated the origin of the subgenus *Trichomycterus* lineage in the early Miocene. The biogeographical analysis performed by Vilardo et al. (2023) indicated that the MRCA of the subgenus *Trichomycterus* inhabited an ancestral area comprising only the Rio Paraíba do Sul, contrasting with its present distribution that includes both this basin and smaller coastal basins (Fig. 4; Costa 2021). However, geological data support a Cenozoic configuration of the RPSB different from the present one, in which its lower course corresponded to the present lower course of the Rio São João (Riccomini et al. 2010), which is now an isolated coastal basin. Thus, geological data are congruent with the hypothesised ancestral area of the subgenus in the Rio Paraíba do Sul alone, which in the past did not include the present upper course but included a present coastal basin in its lower course. The upper course of the RPSB probably was blocked for dispersion of trichomycterine catfishes that live in fast flowing streams by the great depression in its main channel responsible for the formation of the paleolake Tremembé during the Oligocene (Riccomini et al. 2004). Thus, it is possible that these two subgenera lineages, *Paracambeva* and *Trichomycterus*, were not in contact in the upper Rio Paraíba do Sul before the Middle Miocene. The origin of the specific colour pattern shared by the syntopic *T. antiquus* and *T. maculosus* is estimated to have occurred first in the *T. itatiayae* group during the Middle Miocene and much later in *T. maculosus* during the Late Pliocene in *T. maculosus*, which is compatible with the hypothesis of a more recent occupation of the upper RPSB by the subgenus *Trichomycterus*.

Interestingly, the other case involving similarly coloured syntopic species of trichomycterines from eastern South America involves *T. itatiayae*, the sister group of *T. antiquus*, and *T. nigroauratus*, the sister group of *T. maculosus* (Fig. 5). These two species are endemic to streams of the RPSB draining the Serra da Mantiqueira and the adjacent Serra da Bocaina (Barbosa and Costa 2008) and are commonly found associated with bottom leaf litter (Costa 2021). Juvenile specimens of these species share a colour pattern consisting of a broad black longitudinal stripe along the flank midline, whereas larger specimens assume a different colour pattern (Barbosa and Costa 2008). A broad black longitudinal stripe is present in all other species of *Paracambeva* (Costa and Katz 2021; Costa et al. 2023b), therefore already present in the

MRCA of this subgenus, whereas this colour pattern is present in part of the species of the *T. nigroauratus* group among species of the subgenus *Trichomycterus* (Costa et al. 2022), thus arising after the initial diversification of this group. Considering the estimated age of *Paracambeva* in the Late Oligocene and the initial diversification of the *T. nigroauratus* group in the Late Pliocene, over 20 million years later, the most plausible hypothesis is that the colour pattern in the *T. nigroauratus* group had arisen after this group was in contact with species of *Paracambeva* in RPSB.

Possible explanations for the occurrence of syntopic trichomycterines with similar colour patterns

The sympatric occurrence of distantly related species of Neotropical catfishes exhibiting similar derived colour patterns has been often aprioristically considered as primary evidence of mimetic association (Axenrot and Kullander 2003; Alexandrou et al. 2011; Slobodian and Bockmann 2013), but may also be a result of evolutionary convergence for adaptation to live in special habitats like those occurring among sympatric psammophilic species (Zuanon et al. 2006; Costa et al. 2020c). Therefore, the occurrence of two species of *Trichomycterus* in the same habitat sharing the same colour pattern (Figs 1A, 6) but belonging to two distantly related subgenera could suggest a case of mimetic association or convergence for adaptation to live in a gravel bottom where both species were found, since their colour pattern is cryptic in this habitat. However, direct evidence to explain syntopic trichomycterines with similar colour patterns is not available for any of these hypotheses.

In the case of evolutionary convergence for adaptation to live in special habitats, a possible explanation is that the colour pattern gives these two species some cryptic advantage in their habitat against predators since the colours are similar to the gravel substrate where they live. In the case of mimetic associations, including both Batesian and Müllerian mimicry, the model species (Batesian) or both species (Müllerian) have effective anti-predation features, which among catfishes usually comprise venom glands associated with fin spines (Wright 2009; Harris and Jenner 2019). For example, in mimetic associations involving siluroids with a well-developed pectoral-fin spine, the main anti-predation morpho-physiological attribute is the presence of an axillary venom gland associated with a pungent pectoral-fin spine (e.g., Greven et al. 2006; Wright 2011; Carvalho et al. 2021). The defence mechanism involves not only glands and the pectoral-fin spine but also special muscles and connective tissue (Wright 2015; Harris and Jenner 2019). However, mechanisms for anti-predation in trichomycterines are still unknown, and potential trichomycterine predators living in the Rio do Peixe drainage have not been presently recorded, although the Neotropical otter *Lontra longicaudis* (Olfers, 1818) and the catfish *Steindachneridion parahybae* (Steindachner, 1877) today rare or absent in the region, were until recently potential predators.

Although anti-predation features consisting of venom glands associated with fin spines occur in most catfish lineages (Wright 2009, 2015), they are unknown among trichomycterids. Unlike other catfishes, trichomycterids do not have pectoral and dorsal spines. In a survey on the presence of venom axillary glands in catfish lineages, Wright (2009) did not detect them in *'Trichomycterus' areolatus* Valenciennes, 1846, concluding that these glands are not present in trichomycterids. However, a supposed axillary gland (e.g., Eigenmann 1918) or suprapectoral adipose organ according to Myers and Weitzman (1966) and axillary organ according to de Pinna (1989), situated at the same place as the venom axillary glands of other catfishes and having a similar orifice, have been superficially described for candirus and other trichomycterids (e.g., Eigenmann 1918). This supposed axillary gland, comprising a sack-like protuberance above the pectoral fin and just below the anterior pores of the lateral line of the flank, is also present in trichomycterines (Fig. 2), which is proportionally smaller than in other trichomycterids (e.g., sarcoglanidines, Myers and Weitzman 1966), with an orifice that is more conspicuous in juvenile specimens below about 40 mm SL, often having a great concentration of melanophores around its margin. Both *T. antiquus* and *T. maculosus* have a small axillary gland-like protuberance below the short lateral line canal and above the pectoral fin (Fig. 2). The absence of a pectoral spine in trichomycterids also imposes a limitation on the possibility of the axillary organ acting as a venom gland. Nonetheless, the stinging action of the opercular odontodes, which are located close to the ax-

Figure 6. *Trichomycterus* (*Trichomycterus*) *maculosus*, UFRJ 13676, 97.6 mm SL, left lateral view.

illary gland-like protuberance (Fig. 2) and may become bristly when the fish is molested, could be performed as the pectoral spine of other catfishes. However, a more detailed morphological study at the histological and biochemical level is necessary to investigate the presence of glandular tissue and toxic substances in *T. antiquus* and close relatives, which is not presently possible with the small sample of specimens currently available. Future studies are necessary to check what hypothesis best explains the unexpected syntopic occurrence of similarly coloured *T. antiquus* and *T. maculosus*.

Acknowledgements

Thanks are due to Léia C. Medeiros, Gustavo L. Canella, and Ronaldo dos Santos-Junior for field assistance. We are also grateful for the comments and criticisms provided by F. Langeani, H.H. Ng, F. Ottoni, and an anonymous reviewer, who contributed to improving the present version of the manuscript. The Instituto Chico Mendes de Conservação da Biodiversidade provided collecting permits. This work was partially supported by the Conselho Nacional de Desenvolvimento Científico e Tecnológico (CNPq; grant 304755/2020-6 to WJEMC) and Fundação Carlos Chagas Filho de Amparo à Pesquisa do Estado do Rio de Janeiro (FAPERJ; grant E-26/201.213/2021 to WJEMC, E-26/202.005/2020 to AMK, and E-26/203.524/2023 to JLM). This study was also supported by CAPES (Finance Code 001) through the Programa de Pós-Graduação em Biodiversidade e Biologia Evolutiva/UFRJ and the Programa de Pós-Graduação em Genética/UFRJ.

References

Alexandrou MA, Oliveira C, Maillard M, McGill RAR, Newton J, Creer S, Taylor MI (2011) Competition and phylogeny determine community structure in Müllerian co-mimics. Nature 469(7328): 249–272. https://doi.org/10.1038/nature09660

Arratia G, Huaquin L (1995) Morphology of the lateral line system and of the skin of diplomystid and certain primitive loricarioid catfishes and systematic and ecological considerations. Bonner Zoologische Monographien 36: 1–110.

Arratia G, Chang A, Menu-Marque S, Rojas G (1978) About *Bullockia* gen. nov., *Trichomycterus mendozensis* n. sp. and revision of the family Trichomycteridae (Pisces, Siluriformes). Studies on Neotropical Fauna and Environment 13(3–4): 157–194. https://doi.org/10.1080/01650527809360539

Axenrot TE, Kullander SO (2003) *Corydoras diphyies* (Siluriformes: Callichthyidae) and *Otocinclus mimulus* (Siluriformes: Loricariidae), two new species of catfishes from Paraguay, a case of mimetic association. Ichthyological Exploration of Freshwaters 14: 249–272.

Barbosa MA, Costa WJEM (2008) Description of a new species of catfish from the upper Rio Paraíba do Sul basin, south-eastern Brazil (Teleostei: Siluriformes: Trichomycteridae) and re-description of *Trichomycterus itatiayae*. Aqua International Journal of Ichthyology 14: 175–186.

Barbosa MA, Costa WJEM (2010) Description of a new species of the catfish genus *Trichomycterus* (Teleostei: Siluriformes: Trichomycteridae) from the RPSB, southeastern Brazil. Vertebrate Zoology 60(3): 193–197. https://doi.org/10.3897/vz.60.e31010

Betancur-R R, Órti G, Pyron RA (2015) Fossil-based comparative analyses reveal ancient marine ancestry erased by extinction in ray-finned fishes. Ecology Letters 18(5): 441–450. https://doi.org/10.1111/ele.12423

Bockmann FA, Sazima I (2004) *Trichomycterus maracaya*, a new catfish from the upper rio Paraná, southeastern Brazil (Siluriformes: Trichomycteridae), with notes on the *T. brasiliensis* species-complex. Neotropical Ichthyology 2(2): 61–74. https://doi.org/10.1590/S1679-62252004000200003

Carvalho TI, Klaczko J, Slobodian V (2021) Pectoral-fin glands and delivery apparatus in the catfish genus *Brachyrhamdia* Myers, 1927 (Siluriformes: Heptapteridae). Papéis Avulsos de Zoologia 61: e20216174. https://doi.org/10.11606/1807-0205/2021.61.74

Chenna R, Sugawara H, Koike T, Lopez R, Gibson TJ, Higgins DG, Thompson JD (2003) Multiple sequence alignmentwith the Clustal series of programs. Nucleic Acids Research 31(13): 3497–3500. https://doi.org/10.1093/nar/gkg500

Costa WJEM (1992) Description de huit nouvelles espèces du genre *Trichomycterus* (Siluriformes: Trichomycteridae), du Brésil oriental. Revue Française d'Aquariologie et Herpetologie 18: 101–110.

Costa WJEM (2021) Comparative osteology, phylogeny and classification of the eastern South American catfish genus *Trichomycterus* (Siluriformes: Trichomycteridae). Taxonomy 1(2): 160–191. https://doi.org/10.3390/taxonomy1020013

Costa WJEM, Katz AM (2021) Integrative taxonomy supports high species diversity of south-eastern Brazilian mountain catfishes of the *T. reinhardti* group (Siluriformes: Trichomycteridae). Systematics and Biodiversity 19(6): 601–621. https://doi.org/10.1080/14772000.2021.1900947

Costa WJEM, Mattos JLO, Amorim PF, Vilardo PJ, Katz AM (2020a) Relationships of a new species support multiple origin of melanism in *Trichomycterus* from the Atlantic Forest of south-eastern Brazil (Siluriformes: Trichomycteridae). Zoologischer Anzeiger 288: 74–83. https://doi.org/10.1016/j.jcz.2020.07.004

Costa WJEM, Katz AM, Mattos JLO, Amorim PF, Mesquita BO, Vilardo PJ, Barbosa MA (2020b) Historical review and redescription of three poorly known species of the catfish genus *Trichomycterus* from south-eastern Brazil (Siluriformes: Trichomycteridae). Journal of Natural History 53(47–48): 2905–2928. https://doi.org/10.1080/00222933.2020.1752406

Costa WJEM, Henschel E, Katz AM (2020c) Multigene phylogeny reveals convergent evolution in small interstitial catfishes from the Amazon and Atlantic forests (Siluriformes: Trichomycteridae). Zoologica Scripta 49(2): 159–173. https://doi.org/10.1111/zsc.12403

Costa WJEM, Mattos JLO, Lopes S, Amorim PF, Katz AM (2022) Integrative taxonomy, distribution and ontogenetic colouration change in Neotropical mountain catfishes of the *Trichomycterus nigroauratus* Group (Siluriformes, Trichomycteridae). Zoological Studies (Taipei, Taiwan) 61: 11. https://doi.org/10.6620/ZS.2022.61-11

Costa WJEM, Mattos JLO, Amorim PF, Mesquita BO, Katz AM (2023a) Chromatic polymorphism in *Trichomycterus albinotatus* (Siluriformes, Trichomycteridae), a mountain catfish from south-eastern Brazil and the role of colouration characters in trichomycterine taxonomy. Zoosystematics and Evolution 99(1): 161–171. https://doi.org/10.3897/zse.99.98341

Costa WJEM, Azevedo-Santos VM, Mattos JLO, Katz AM (2023b) Molecular phylogeny, taxonomy and distribution patterns of trichomycterine catfishes in the middle Rio Grande drainage, south-eastern Brazil (Siluriformes: Trichomycteridae). Fishes 8(4): 206. https://doi.org/10.3390/fishes8040206

da Silva CCF, da Matta SLSF, Hilsdorf AWS, Langeani F, Marceniuk AP (2010) Color pattern variation in *Trichomycterus iheringi* (Eigenmann, 1917) (Siluriformes: Trichomycteridae) from rio Itatinga and rio Claro, São Paulo, Brazil. Neotropical Ichthyology 8(1): 49–56. https://doi.org/10.1590/S1679-62252010000100007

de Pinna MCC (1989) A new sarcoglandine catfish, phylogeny of its subfamily, and an appraisal of the phyletic status of the Trichomycterinae (Teleostei, Trichomycteridae). American Museum Novitates 2950: 1–39.

Eigenmann CH (1918) The Pygidiidae, a family of South American catfishes. Memoirs of the Carnegie Museum 7(5): 259–398. https://doi.org/10.5962/p.34486

Gernhard T (2008) The conditioned reconstruction process. Journal of Theoretical Biology 253(4): 769–778. https://doi.org/10.1016/j.jtbi.2008.04.005

Greven H, Flasbeck T, Passia D (2006) Axillary glands in the armoured catfish *Corydoras aeneus* (Callichthyidae, Siluriformes). Verhandlungen der Gesellschaft für Ichthyologie 5: 65–69.

Guindon S, Dufayard JF, Lefor V, Anisimova M, Hordijk W, Gascuel O (2010) New algorithms and methods to estimate maximum-likelihood phylogenies: Assessing the performance of PhyML 3.0. Systematic Biology 59(3): 307–321. https://doi.org/10.1093/sysbio/syq010

Harris RJ, Jenner RA (2019) Evolutionary ecology of fish venom: Adaptations and consequences of evolving a venom system. Toxins 11(2): 60. https://doi.org/10.3390/toxins11020060

Hoang DT, Chernomor O, von Haeseler A, Minh BQ, Vinh LS (2018) UFBoot2: Improving the ultrafast bootstrap approximation. Molecular Biology and Evolution 35(2): 518–522. https://doi.org/10.1093/molbev/msx281

King LC (1956) A Geomorfologia do Brasil Oriental. Revista Brasileira de Geografia 18: 147–265.

Kubicek KM (2022) Developmental osteology of *Ictalurus punctatus* and *Noturus gyrinus* (Siluriformes: Ictaluridae) with a discussion of siluriform bone homologies. Vertebrate Zoology 72: 661–727. https://doi.org/10.3897/vz.72.e85144

Lanfear R, Frandsen PB, Wright AM, Senfeld T, Calcott B (2016) PartitionFinder 2: New methods for selecting partitioned models of evolution for molecular and morphological phylogenetic analyses. Molecular Biology and Evolution 34: 772–773. https://doi.org/10.1093/molbev/msw260

Minh BQ, Schmidt HA, Chernomor O, Schrempf D, Woodhams MD, von Haeseler A, Lanfear R (2020) IQ-TREE 2: New models and efficient methods for phylogenetic inference in the genomic era. Molecular Biology and Evolution 37(5): 1530–1534. https://doi.org/10.1093/molbev/msaa015

Myers GS, Weitzman SH (1966) Two remarkable new trichomycterid catfishes from the Amazon basin in Brazil and Colombia. Journal of Zoology (London, England) 149(3): 277–287. https://doi.org/10.1111/j.1469-7998.1966.tb04049.x

Ochoa LE, Roxo FF, DoNascimiento C, Sabaj MH, Datovo A, Alfaro M, Oliveira C (2017) Multilocus analysis of the catfish family Trichomycteridae (Teleostei: Ostariophysi, Siluriformes) supporting a monophyletic Trichomycterinae. Molecular Phylogenetics and Evolution 115: 71–81. https://doi.org/10.1016/j.ympev.2017.07.007

Price AC, Weadick CJ, Shim J, Rodd FH (2008) Pigments, Patterns, and Fish Behavior. Zebrafish 5(4): 297–307. https://doi.org/10.1089/zeb.2008.0551

Rambaut A, Drummond AJ, Xie D, Baele G, Suchard MA, Rambaut A, Drummond AJ, Xie D, Baele G, Suchard MA (2018) Posterior summarisation in Bayesian phylogenetics using Tracer 1.7. Systematic Biology 67(5): 901–904. https://doi.org/10.1093/sysbio/syy032

Reis VJC, dos Santos SA, Britto MR, Volpi TA, de Pinna MCC (2020) Iterative taxonomy reveals a new species of *Trichomycterus* Valenciennes 1832 (Siluriformes, Trichomycteridae) widespread in Rio Doce Basin: A pseudocryptic of *T. immaculatus*. Journal of Fish Biology 97(6): 1607–1623. https://doi.org/10.1111/jfb.14490

Rezende EA, Salgado AAR, Castro PTA (2018) Evolução da rede de drenagem e evidências de antigas conexões entre as bacias dos rios Grande e São Francisco no sudeste brasileiro. Revista Brasileira de Geomorfologia 19(3): 483–501. https://doi.org/10.20502/rbg.v19i3.1304

Riccomini C, Sant'Anna LG, Ferrari AL (2004) Evolução geológica do Rift Continental do Sudeste do Brasil. In: Mantesso-Neto V, Bartorelli A, Carneiro CDR, Brito-Neves BB (Eds) Geologia do continente Sul-Americano: evolução da obra de Fernando Flávio Marques de Almeida. Beca, São Paulo, 383–405.

Riccomini C, Grohmann CH, Sant'Anna LG, Hiruma ST (2010) A captura das cabeceiras do Rio Tietê pelo Rio Paraíba do Sul. In: Modenesi-Gauttieri MC, Bartorelli A, Mantesso-Neto V, Carneiro CDR, Lisboa MBAL (Eds) A obra de Aziz Nacib Ab'Sáber. Beca, São Paulo, 157–169.

Sarmento-Soares LM, Martins-Pinheiro RF, Aranda AT, Chamon CC (2005) *Trichomycterus pradensis*, a new catfish from southern Bahia coastal rivers, northeastern Brazil (Siluriformes: Trichomycteridae). Ichthyological Exploration of Freshwaters 16: 289–302.

Slobodian V, Bockmann FA (2013) A new *Brachyrhamdia* (Siluriformes: Heptapteridae) from Rio Japurá basin, Brazil, with comments on its phylogenetic affinities, biogeography and mimicry in the genus. Zootaxa 3717(1): 1–22. https://doi.org/10.11646/zootaxa.3717.1.1

Suchard MA, Lemey P, Baele G, Ayres DL, Drummond AJ, Rambaut A (2018) Bayesian phylogenetic and phylodynamic data integration using BEAST 1.10. Virus Evolution 4(1): vey016. https://doi.org/10.1093/ve/vey016

Tamura K, Stecher G, Kumar S (2021) MEGA11: Molecular Evolutionary Genetics Analysis Version 11. Molecular Biology and Evolution 38(7): 3022–3027. https://doi.org/10.1093/molbev/msab120

Taylor WR, Van Dyke GC (1985) Revised procedures for staining and clearing small fishes and other vertebrates for bone and cartilage study. Cybium 9: 107–119.

Valenciennes A (1832) Nouvelles observations sur le Capitan de Bogota, *Eremophilus mutisii*. In: Humboldt A, Bonpland A (Eds) Recueil d'observations de Zoologie et d'Anatomie Comparée, faites dans l'Ocean Atlantique, dans l'interieur du Nouveau Continent et dans la Mer du Sud pendant les annés 1799, 1800, 1801, 1802 et 1803, deuxième volume. Observations de Zoologie et d'Anatomie comparée, 341–348.

Vilardo PJ, Katz AM, Costa WJEM (2023) Chromatic polymorphism in *Trichomycterus jacupiranga* from eastern Brazilian coastal basins (Siluriformes: Trichomycteridae). Zootaxa 5285(2): 360–372. https://doi.org/10.11646/zootaxa.5285.2.8

Villa-Verde L, Lazzarotto H, Lima SQM (2012) A new glanapterygine catfish of the genus *Listrura* (Siluriformes: Trichomycteridae) from southeastern Brazil, corroborated by morphological and molecular data. Neotropical Ichthyology 10(3): 527–538. https://doi.org/10.1590/S1679-62252012000300005

Ward RD, Zemlak TS, Innes BH, Last PR, Hebert PD (2005) DNA barcoding Australia's fish species. Philosophical Transactions of the Royal Society of London. Series B, Biological Sciences 360(1462): 1847–1857. https://doi.org/10.1098/rstb.2005.1716

Wright JJ (2009) Diversity, phylogenetic distribution, and origins of venomous catfishes. BMC Evolutionary Biology 9(1): 282. https://doi.org/10.1186/1471-2148-9-282

Wright JJ (2011) Conservative coevolution of Mullerian mimicry in a group of rift lake catfish. Evolution; International Journal of Organic Evolution 65(2): 395–407. https://doi.org/10.1111/j.1558-5646.2010.01149.x

Wright JJ (2015) Evolutionary History of Venom Glands in the Siluriformes. In: Gopalakrishnakone P. & Malhotra, A. (Eds.). Evolution of Venomous Animals and Their Toxins. Dordrecht, Springer, 1–19. https://doi.org/10.1007/978-94-007-6727-0_9-1

Zuanon J, Bockmann FA, Sazima I (2006) A remarkable sand-dwelling fish assemblage from central Amazonia, with comments on the evolution of psammophily in South American freshwater fishes. Neotropical Ichthyology 4(1): 107–118. https://doi.org/10.1590/S1679-62252006000100012

Supplementary material 1

List of comparative material of the subgenus *Paracambeva*

Authors: Wilson J. E. M. Costa, Caio R. M. Feltrin, José Leonardo O. Mattos, Axel M. Katz

Data type: pdf

Link: https://doi.org/10.3897/zse.100.118000.suppl1

Supplementary material 2

The independent analysis of individual gene trees

Authors: Wilson J. E. M. Costa, Caio R. M. Feltrin, José Leonardo O. Mattos, Axel M. Katz

Data type: pdf

Link: https://doi.org/10.3897/zse.100.118000.suppl2

Supplementary material 3

Beast divergence-time estimation

Authors: Wilson J. E. M. Costa, Caio R. M. Feltrin, José Leonardo O. Mattos, Axel M. Katz

Data type: pdf

Link: https://doi.org/10.3897/zse.100.118000.suppl3